Thin Solid Films 743 (2022) 139069

Contents lists available at ScienceDirect

Thin Solid Films

journal homepage: www.elsevier.com/locate/tsf

Temperature dependent optical and electrical characterization of SnS/CdS solar cell

Taavi Raadik [a,*], Nicolae Spalatu [a], Jüri Krustok [a,b], Raavo Josepson [b], Maarja Grossberg [a]

[a] Department of Materials and Environmental Technology, Tallinn University of Technology, Ehitajate tee 5, 19086 Tallinn, Estonia
[b] Division of Physics, Tallinn University of Technology, Ehitajate Tee 5, 19086 Tallinn, Estonia

ARTICLE INFO

Keywords:
Solar cells
Electroreflectance, bandgap, tin sulfide

ABSTRACT

The optical and electrical properties of SnS thin film solar cell, manufactured by close spaced sublimation, was studied by electroreflectance spectroscopy, external quantum efficiency and current-voltage characteristics in the temperature range of T = 20–300 K. Temperature dependence of the open circuit voltage indicated to the interface recombination as the main limiting factor for the device performance. Room temperature external quantum efficiency curves of SnS solar cell showed two optical transitions at 1.30 eV and 1.53 eV. These findings contribute to the better understanding of the fundamental properties of SnS as a prospective absorber material for next-generation solar cells.

1. Introduction

There is a continuous search for earth abundant, nontoxic and cheap materials for solar energy conversion. Orthorhombic SnS has all the necessary parameters to be a good absorber material in thin film solar cells, namely p-type conductivity, high absorption coefficient 10^4–10^5 cm^{-1} and a direct optical bandgap of E_g=1.317 eV at room temperature [1–4]. On the other hand SnS bandgap value of E_g=1.1 eV for orthorhombic – and E_g=1.7 eV for cubic crystal structure has been reported [5,6], additionally in SnS an indirect optical transition is possible with band gap energy of 1.07 eV [7]. Despite the fact that the optical and electrical properties of SnS have been studied for a decade, there are still many uncertainties and open questions, especially concerning bandgap energy values and behavior from temperature. Nevertheless, SnS has been defined as a next challenge and breakthrough among emerging solar energy materials as an earth abundant and cheap absorber for photovoltaics (PV). Although the theoretical maximum device efficiency of a SnS solar cell should be 32% [8], experimentally only 4.36% [8] has been obtained, meaning there is still a long way to go. The poor performance of SnS solar cells has been attributed to the weak material quality, band alignment problems and rapid carrier recombination at trap states near the interface between SnS and the n-type buffer layer [9, 10].

Electroreflectance spectroscopy (ER) is a non-destructive and powerful technique to study material's optical properties, it provides an exceptionally precise tool for evaluating the band gap energy of the material. In the studies of SnS solar cells ER hasn't been used before and precise data about the temperature dependence of band gap energy of the absorber in the complete solar cell device is absent in the literature. Thus, the focus of this study was to perform in-depth analysis of temperature dependent optoelectronic properties of SnS thin film solar cell by combining advanced ER and classical current-voltage (I-V-T) and external quantum efficiency (EQE) measurements techniques. The obtained results bring insights into the fundamental properties of the emerging PV absorber material SnS and pave the way to improve the performance of the corresponding solar cell device.

2. Experimental details

Fabrication of SnS solar cells in superstrate configuration included the deposition of the CdS buffer layer onto the fluorine doped tin oxide (FTO) layer, ot top of the glass substrate by close space sublimation (CSS) method from powdered source material with 5 N (99.999%) purity (Alfa Aesar), the completed device structure is as follows glass/FTO/CdS/SnS/Au. The deposition time, source temperature, and substrate temperature for CdS layer were established as 8 min, 590 °C, and 300 °C, respectively. The thickness of CdS layer was approximately 80 nm. Following the deposition sequence, SnS absorber layer of ~1.5 μm thickness was also deposited by CSS (from 4 N granulated SnS source material, Testbourne Ltd). The CSS source temperature, substrate

* Corresponding author.
E-mail address: taavi.raadik@taltech.ee (T. Raadik).

https://doi.org/10.1016/j.tsf.2021.139069
Received 24 August 2021; Received in revised form 17 December 2021; Accepted 17 December 2021
Available online 21 December 2021

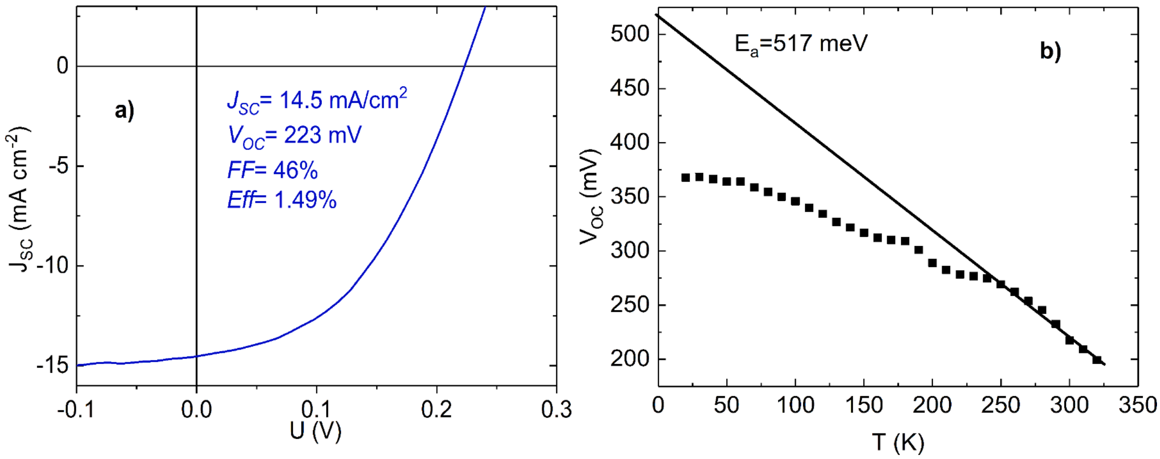

Fig. 1. a) I-V curve of the studied SnS solar cell at room temperature, b) Temperature dependence of the Voc of the SnS solar cell together with a linear fit from the linear part of the slope.

temperature, and deposition time were kept constant at 560 °C, 500 °C, and 2 min, respectively. Prior to evaporation, the SnS source material passed the so-called "standardization" pre-annealing procedure to remove the secondary phases [11]. Typical sheet resistance of the FTO substrate layer was 20 Ω/sq, with a nominal film thickness of 200 nm. To complete the cells, Au back contacts with square geometries (25 mm^2) were deposited by vacuum evaporation through a mica mask placed between the evaporation source and the sample. X-ray diffraction (XRD) measurements were preformed to the CSS deposited SnS film, which confirmed the presence of an orthorhombic SnS, no other phases were detected. Electroreflectance measurements were carried out using traditional set-up [12], where 250 W halogen lamp together with Horiba Jobin Yvon FHR640 monochromator (f = 640 mm) was used for illumination. The spot size of the reflected light was around 1 × 2 mm. At the same time the DC- and AC-voltage were applied to a solar cell under study via back and front contact by a pulse generator with frequency of 223 Hz, AC value of ±0.5 V and DC component of −0.5 V, in order to call out the disruptions in reflectance near the critical points in material. The signal was detected by Si detector and lock-in amplifier (SR 810).

I–V curves were measured using an Autolab PGSTAT system. As a light source we used a standard halogen lamp with calibrated intensity with maximum of 100 mW/cm^2. For external quantum efficiency measurements (EQE) a 100 W calibrated halogen lamp was used as a light source together with the a SPM-2 prism monochromator. Monochromatic and modulated (120 Hz) light was focused on the front surface of the solar cell. The generated short circuit current was detected with a DSP Lock-In amplifier (SR 810). In order to perform temperature dependent measurements of ER, EQE and I-V, the solar cell was mounted on the cold finger of a closed-cycle He cryostat (Janis) and the temperature of the cell was changed from 320 to 20 K with ΔT = 10 K.

3. Results and discussion

The current – voltage I-V curve of the SnS cell at room temperature is presented in Fig. 1a), measured under AM1.5 condition. The solar cell exhibited a conversion efficiency of 1.49% with open-circute voltage 223 mV, short-circuit density 14.5 mA/cm^2 and fill factor 46%.

To detect dominant recombination mechanism in SnS solar cell, the temperature dependent I-V measurements were preformed in the range of 20 – 320 K and under the illumination of 100 mW/cm^2. The temperature dependence of V_{OC} is given in Fig. 1b). As it can be seen, the V_{OC} is following the theoretical trend where with the decrease of the temperature V_{OC} is increasing. The relationship between V_{OC} and T can be described by Eq. 1:

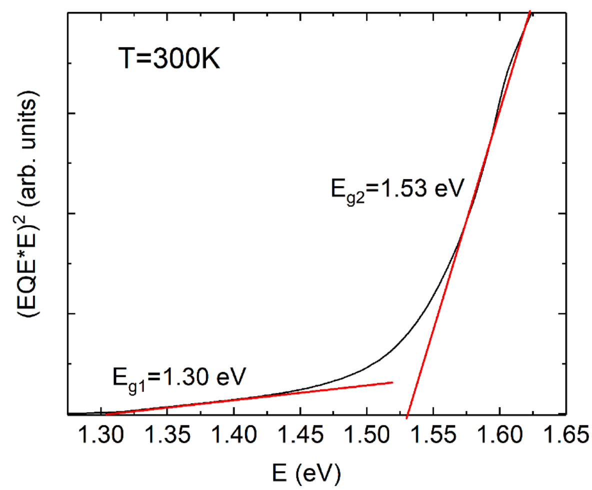

Fig. 2. $(EQE*E)^2$ vs photon energy curve of SnS solar cell at room temperature together with E_{g1} and E_{g2}.

$$V_{oc} = \frac{E_A}{q} - \frac{nkT}{q}\ln\left(\frac{J_{00}}{J_L}\right) \quad (1)$$

where E_A is the activation energy that depends mainly on the dominating recombination mechanism, q is the elementary charge, n is the ideality factor, k is the Boltzmann constant, T is the temperature, J_{00} is the diode reverse saturation current prefactor and J_L is the light generated current density [13,14].

To find the activation energy and to compare it with the band gap energy we need to extrapolate the linear part of the V_{OC} from V_{OC} vs T plot, that is presented on Fig. 1b) in the range of 325 K to 250 K. We found that the activation energy is E_a~517 meV, which is much less than the band gap energy of 1317 meV at 0 K, that is reported in the literature [4]. It is indicating that charge carriers recombination, at least at temperatures around room temperature, according to the theory takes place in the interface region and it could be the main predominant factor for limiting the device performance [13,15–19].

Quantum efficiency measurement is a well-known method to describe optical and electronic losses in solar cell but also estimate the bandgap energy of the absorber material of the device. If we consider SnS as a direct bandgap semiconductor, then from the low energy side of the EQE curve i.e. near the band gap energy $E \approx E_g$, the effective band gap energy E_g* can be determined [20] by using an approximation

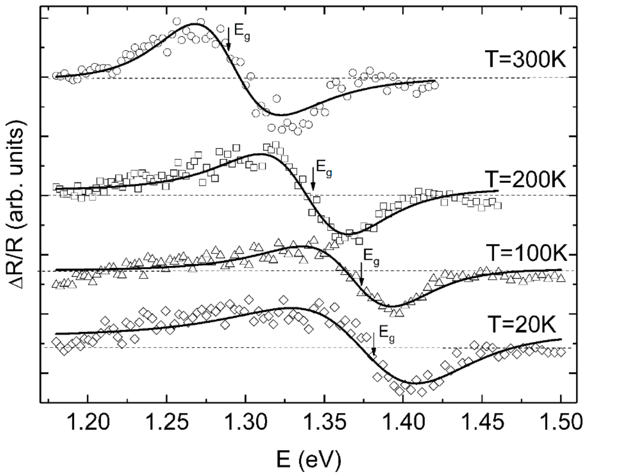

Fig. 3. ER spectra of SnS solar cell at 20 K, 100 K, 200 K and 300 K together with fitting results with Eq. 3.

proposed by Klenk and Schock [21]:

$$EQE \approx K\alpha L_{eff} \approx A\left(E - E_g^*\right)^{1/2} \Big/ E \tag{2}$$

where constant A includes all energy independent parameters, $L_{eff} = w + L_d$ is the effective diffusion length of minority carriers, L_d is their diffusion length in the absorber material, w is the width of the depletion region, and α is the absorption coefficient of the absorber material. The constant K is unity in absolute measurements [22,23]. By plotting $(EQE^*E)^2$ vs E we can detect linear segment, from where it is possible to find the effective band gap energies. As it can be seen on Fig. 2 from the $(EQE^*E)^2$ vs E graph, we can detect two linear sections and after extrapolating these areas on the graphs we can determine the room temperature band gap energies as E_{g1}~1.30 eV and E_{g2}~1.53 eV. Similar behavior, where two absorption edges were detected in SnS, has been also reported by other authors [10,24,25]. As SnS can exist in the form of different polymorphs such as orthorhombic (α-SnS) and cubic structure (π-SnS), it could be possible that both polymorphs are present in our sample, as bandgap of α-SnS ~1,30 eV and bandgap of π-SnS 1.5 - 1.70 eV values have been reported [26,27]. However, the XRD measurements showed only a presence of orthorhombic SnS phase in our films, but it could be possible that cubic SnS phase exists in such a tiny amount in the film and it is located in the interface area, so that XRD is not able to detect it. Co-existence of different polymorphs is nothing unusual in chalcogenides [28]. However, there is still no clear understanding about the origin of E_{g2} in SnS, meaning more future studies are needed for clarification. To evaluate the temperature dependent bandgap behavior, we preformed EQE measurmenst in the range of 20–300 K.

Electroreflectance is one type of modulation spectroscopy, where the external AC voltage is applied to the structure with a pulse generator in order to modulate internal electric field within the region of the junction. The applied voltage leads to a carrier redistribution, which influences the internal electric field inside the sample and causes a change of the dielectric function in the space charge region. Therefore, the reflectivity R of the studied heterostructure varies with the applied AC voltage and the change between the reflectivity coefficients is visible in the measured reflectance spectrum as a sharp derivative feature near the critical points [29].

All electroreflectance spectra measured at different temperatures were fitted with a Aspenes third-derivative functional form [30]

$$\Delta R/R = Re\left[Ae^{i\varphi}\left(E - E_g + i\Gamma\right)^{-m}\right] \tag{3}$$

where E is the photon energy, A corresponds to the amplitude, φ is the phase, E_g value of band gap energy and Γ broadening parameter of the spectrum. Parameter m is defined by the type of the critical point, $m = 2.5$ was used in our study. It corresponds to the three dimensional critical point that is related to interband transition between the conduction-band minimum and valence-band maximum [30]. Experimental results together with fittings can be seen on Fig. 3. It is clearly seen that the band gap energy of SnS shifts toward the lower energy with increasing temperature. Interestingly, the gamma value (Γ) or broadening parameter, which is usually related to structural and compositional disorders in the material and classically drops with the decrease of the temperature showed an abnormal behavior. It stayed practically constant with the value of Γ ~ 60 meV within the temperature range of 300–50 K and slightly increased for the temperatures below 50 K. Such a abnormal behavior of broadering parameter has been seen in other chalcogenide PV materials [31,32]. Krustok et al. [31] explained this phenome could be related to the presence of potential and band gap energy fluctuations in kesterite materials. It is well known fact that ordered and disordered kesterite structure can be present in the material [33–35] that cause the bandgap fluctuation, in addition different defect clusters could be the reason for localized bandgap decreasing [36]. In SnS bandgap fluctuations could be related to the high concentration of native point defects, similar phenome has been reported in other binary compound [37], main defects in SnS are Sulphur vacancies [11] that most probably will cause the inhomogeneous broadening of ER spectra.

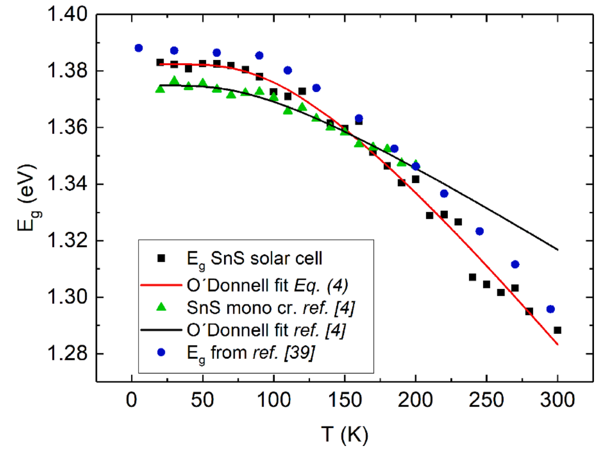

Fig. 4. Temperature dependent bandgap shifting behavior according to ER data from current study together with fitting with Eq. (4) and comparison with SnS monocrystal PR data [4] and polycrystal absorption data [39].

Table 1
Fitting parameters of temperature dependent bandgap shifting with Eq. (4).

Parameter	ODonnell fit E_{g1} (EQE)	ODonnell fit E_{g2} (EQE)	ODonnell fit E_g (ER)
$E_g(0)$ (eV)	1.394 ± 0.001	1.590 ± 0.002	1.382 ± 0.001
S	2.4 ± 0.1	1.1 ± 0.1	3.7 ± 0.3
<ħω> meV	16.6 ± 2	41.3 ± 2.3	31.1 ± 0.3

The temperature dependence of the band gap energy found from fittings, together with fitting curves with ODonnell expression [38] (Eq. (4)), can be seen on Fig. 4.

O'Donnell expression [38] is given as

$$E_g(T) = E_g(0) - S\langle\hbar\omega\rangle[\coth(\langle\hbar\omega\rangle / 2kT) - 1] \tag{4}$$

where $E_g(0)$ is the band gap energy at 0 K, S is a dimensionless coupling constant and <ħω> represents an average phonon energy. Obtained fitting parameters are presented in Table 1.

The temperature dependent behavior of the band gap energy of the polycrystalline SnS thin film is a bit different from the behavior of the

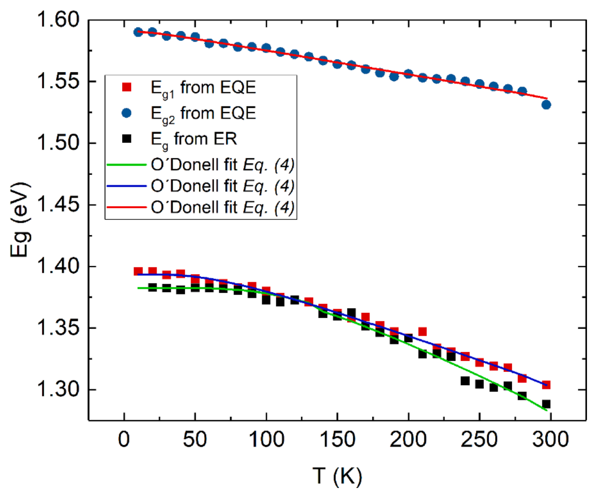

Fig. 5. Temperature dependence of band gap energies found from EQE fits, together with band gap energies found from ER and fittings with Eq. 4.

SnS single crystals photoreflectance (PR) data, as we have previously reported [4], but almost identical to what was reported by Parenteau et al. [39]. However, band gap enrgy values obtained from the current study are a bit smaller and the change from temperature is more pronounced, compared to the study by Parenteau et al. [39], see Fig. 4.

Interestingly, we were not able to detect the second bandgap around 1.6 eV, contractitinally to the EQE measurments, from the electroreflectance, that is the reason why the ER spectra are presented up to 1.49 eV.

Temperature dependent effective band gap energies, found with $(EQE^*E)^2$ method, together with the band gap energy detected from electroreflectance and fittings with Eq. (4), are presented in Fig.5. Effective band gap energy is following the trend of bandgap obtained by ER, nevertheless, there is a slight mismatch at low and high temperatures but it is in the range of measurements error. Fitting parameters of the curves can be found in Table 1.

The Voc temperature dependent measurements indicates to the interface recombination as dominant limitation of the device performance. However inhomogeneous broadening of the ER spectra from the temperature, suggest that interface recombination might be not the only limiting factor and the bulk recombination (due to the high density of the charged defects) still have a significant contribution. This results suggest that more research effort should be put on optimization of both absorber - buffer interface as well as the absorber itself.

4. Conclusions

In this work, we performed a detailed analysis of the optoelectronic properties of close spaced sublimated SnS thin film solar cells using temperature-dependent ER, EQE, and I-V-T characteristics. It was found that the band gap energy of SnS absorber layer changed from 1.38 eV to 1.28 eV with the increase of temperature from 20 K to 300 K. EQE response of the device showed the presence of two absorption edges, E_{g1}~1.30 eV and E_{g2}~1.53 eV at room temperature, that could be related to co-existence of both orthorhombic and cubic polymorphs of SnS. The activation energy E_a~517 meV, determined from V_{OC} temperature dependence, indicated to the interface recombination as the main predominant factor for limiting the device performance. Nevertheless inhomogenius broadering of ER spectra from temeprature indicating contribution of bulk recombination, due to the high density of the charged defects, that have a contribution to the poor device performance.

CRediT authorship contribution statement

Taavi Raadik: Writing – original draft, Writing – review & editing, Investigation, Funding acquisition, Project administration. **Nicolae Spalatu:** Writing – original draft, Writing – review & editing, Investigation, Formal analysis. **Jüri Krustok:** Writing – original draft, Investigation. **Raavo Josepson:** Investigation, Formal analysis. **Maarja Grossberg:** Writing – original draft, Supervision, Funding acquisition, Project administration.

Declaration of Competing Interest

The authors declare that they have no known competing financial interests or personal relationships that could have appeared to influence the work reported in this paper.

Acknowledgments

This work has been supported by the European Regional Development Fund, Project TK141, Estonian Research Council project PRG1023, PRG627, PSG689, the EU H2020 program under the ERA Chair project 5GSOLAR grant agreement No 952509 and Mobilitas Pluss Returning Researcher Grant MOBTP131.

References

[1] J.Y. Kim, S.M. George, Tin monosulfide thin films grown by atomic layer deposition using tin 2,4-pentanedionate and hydrogen sulfide, J. Phys. Chem. C. (2010), https://doi.org/10.1021/jp9120244.

[2] N. Koteeswara Reddy, Y.B. Hahn, M. Devika, H.R. Sumana, K.R. Gunasekhar, Temperature-dependent structural and optical properties of SnS films, J. Appl. Phys. (2007), https://doi.org/10.1063/1.2729450.

[3] C. Gao, H. Shen, L. Sun, Z. Shen, Chemical bath deposition of SnS films with different crystal structures, Mater. Lett. (2011), https://doi.org/10.1016/j.matlet.2011.02.017.

[4] T. Raadik, M. Grossberg, J. Raudoja, R. Traksmaa, J. Krustok, Temperature-dependent photoreflectance of SnS crystals, J. Phys. Chem. Solids. 74 (2013) 1683–1685, https://doi.org/10.1016/j.jpcs.2013.06.002.

[5] N. Koteeswara Reddy, M. Devika, E.S.R. Gopal, Review on tin (II) sulfide (SnS) material: synthesis, properties, and applications, Crit. Rev. Solid State Mater. Sci. (2015), https://doi.org/10.1080/10408436.2015.1053601.

[6] A.R. Garcia-Angelmo, R. Romano-Trujillo, J. Campos-Álvarez, O. Gomez-Daza, M. T.S. Nair, P.K. Nair, Thin film solar cell of SnS absorber with cubic crystalline structure, Phys. Status Solidi Appl. Mater. Sci. (2015), https://doi.org/10.1002/pssa.201532405.

[7] J. Vidal, S. Lany, M. D'Avezac, A. Zunger, A. Zakutayev, J. Francis, J. Tate, Band-structure, optical properties, and defect physics of the photovoltaic semiconductor SnS, Appl. Phys. Lett. (2012), https://doi.org/10.1063/1.3675880.

[8] P. Sinsermsuksakul, L. Sun, S.W. Lee, H.H. Park, S.B. Kim, C. Yang, R.G. Gordon, Overcoming efficiency limitations of SnS-based solar cells, Adv. Energy Mater. (2014), https://doi.org/10.1002/aenm.201400496.

[9] H.S. Yun, B. wook Park, Y.C. Choi, J. Im, T.J. Shin, S. Il Seok, Efficient nanostructured TiO2/SnS heterojunction solar cells, Adv. Energy Mater. 9 (2019) 1–7, https://doi.org/10.1002/aenm.201901343.

[10] P. Sinsermsuksakul, K. Hartman, S. Bok Kim, J. Heo, L. Sun, H. Hejin Park, R. Chakraborty, T. Buonassisi, R.G. Gordon, Enhancing the efficiency of SnS solar cells via band-offset engineering with a zinc oxysulfide buffer layer, Appl. Phys. Lett. 102 (2013) 1–5, https://doi.org/10.1063/1.4789855.

[11] N. Spalatu, J. Hiie, R. Kaupmees, O. Volobujeva, J. Krustok, I.O. Acik, M. Krunks, Postdeposition processing of SnS thin films and solar cells: prospective strategy to obtain large, sintered, and doped sns grains by recrystallization in the presence of a metal halide flux, ACS Appl. Mater. Interfaces. (2019), https://doi.org/10.1021/acsami.9b03213.

[12] T. Raadik, J. Krustok, R. Josepson, J. Hiie, T. Potlog, N. Spalatu, Temperature dependent electroreflectance study of CdTe solar cells, Thin Solid Films 535 (2013) 279–282, https://doi.org/10.1016/j.tsf.2012.12.083.

[13] J. Krustok, R. Josepson, M. Danilson, D. Meissner, Temperature dependence of Cu2ZnSn(SexS1-x)4 monograin solar cells, Sol. Energy. (2010), https://doi.org/10.1016/j.solener.2009.09.011.

[14] S. Oueslati, M. Grossberg, M. Kauk-Kuusik, V. Mikli, K. Ernits, D. Meissner, J. Krustok, Effect of germanium incorporation on the properties of kesterite Cu2ZnSn(S,Se)4 monograins, Thin Solid Films (2019), https://doi.org/10.1016/j.tsf.2018.11.020.

[15] N. Spalatu, R. Krautmann, A. Katerski, E. Karber, R. Josepson, J. Hiie, I.O. Acik, M. Krunks, Screening and optimization of processing temperature for Sb2Se3 thin film growth protocol: interrelation between grain structure, interface intermixing and solar cell performance, Sol. Energy Mater. Sol. Cells. (2021), https://doi.org/10.1016/j.solmat.2021.111045.

[16] S. Oueslati, M. Kauk-Kuusik, C. Neubauer, V. Mikli, D. Meissner, G. Brammertz, B. Vermang, J. Krustok, M. Grossberg, Study of $(Ag_xCu_{1-x})_2ZnSn(S,Se)_4$ monograins synthesized by molten salt method for solar cell applications, Sol. Energy. (2020), https://doi.org/10.1016/j.solener.2020.02.002.

[17] K. Timmo, M. Altosaar, M. Pilvet, V. Mikli, M. Grossberg, M. Danilson, T. Raadik, R. Josepson, J. Krustok, M. Kauk-Kuusik, The effect of Ag alloying of $Cu_2(Zn,Cd)SnS_4$ on the monograin powder properties and solar cell performance, J. Mater. Chem. A. (2019), https://doi.org/10.1039/c9ta07768e.

[18] R. Scheer, Activation energy of heterojunction diode currents in the limit of interface recombination, J. Appl. Phys. (2009), https://doi.org/10.1063/1.3126523.

[19] V. Nadenau, U. Rau, A. Jasenek, H.W. Schock, Electronic properties of $CuGaSe_2$-based heterojunction solar cells. Part I. Transport analysis, J. Appl. Phys. (2000), https://doi.org/10.1063/1.371903.

[20] J. Krustok, R. Josepson, T. Raadik, M. Danilson, Potential fluctuations in $Cu_2ZnSnSe_4$ solar cells studied by temperature dependence of quantum efficiency curves, Phys. B Condens. Matter. (2010), https://doi.org/10.1016/j.physb.2010.04.041.

[21] R. Klenk, H.-.W. Schock, Photocurrent Collection in Thin Film Solar Cells - Calculation and Characterisation for $CuGaSe_2$/(Zn,Cd), in: Proc. 12th Eur. PVSE, 1994, pp. 1588–1591.

[22] M. Danilson, E. Kask, N. Pokharel, M. Grossberg, M. Kauk-Kuusik, T. Varema, J. Krustok, Temperature dependent current transport properties in Cu_2ZnSnS_4solar cells, Thin Solid Films (2015), https://doi.org/10.1016/j.tsf.2014.10.069.

[23] M. Richter, M.S. Hammer, T. Sonnet, J. Parisi, Bandgap extraction from quantum efficiency spectra of $Cu(In,Ga)Se_2$ solar cells with varied grading profile and diffusion length, Thin Solid Films (2017), https://doi.org/10.1016/j.tsf.2016.08.022.

[24] D. Lim, H. Suh, M. Suryawanshi, G.Y. Song, J.Y. Cho, J.H. Kim, J.H. Jang, C. W. Jeon, A. Cho, S.J. Ahn, J. Heo, Kinetically controlled growth of phase-pure SnS absorbers for thin film solar cells: achieving efficiency near 3% with long-term stability using an SnS/CdS heterojunction, Adv. Energy Mater. (2018), https://doi.org/10.1002/aenm.201702605.

[25] J.Y. Cho, S.Y. Kim, R. Nandi, J. Jang, H.S. Yun, E. Enkhbayar, J.H. Kim, D.K. Lee, C. H. Chung, J.H. Kim, J. Heo, Achieving over 4% efficiency for SnS/CdS thin-film solar cells by improving the heterojunction interface quality, J. Mater. Chem. A. (2020), https://doi.org/10.1039/d0ta06937j.

[26] T.R. Rana, S.Y. Kim, J.H. Kim, Existence of multiple phases and defect states of SnS absorber and its detrimental effect on efficiency of SnS solar cell, Curr. Appl. Phys. (2018), https://doi.org/10.1016/j.cap.2018.03.024.

[27] K.J. Norton, F. Alam, D.J. Lewis, A review of the synthesis, properties, and applications of bulk and two-dimensional Tin (II) sulfide (SnS), Appl. Sci. (2021), https://doi.org/10.3390/app11052062.

[28] T. Raadik, M. Grossberg, J. Krustok, M. Kauk-Kuusik, A. Crovetto, R. Bolt Ettlinger, O. Hansen, J. Schou, Temperature dependent photoreflectance study of Cu_2SnS_3 thin films produced by pulsed laser deposition, Appl. Phys. Lett. (2017), https://doi.org/10.1063/1.4990657.

[29] F..H. Pollak, Modulation spectroscopy of semiconductors and semiconductor microstructures, in: M. Balanski (Ed.), Handb. Semicond., Ed., North- Holland Publishing Company, Amsterdam, 1994, p. 527.

[30] D.E. Aspnes, Third-derivative modulation spectroscopy with low-field electroreflectance, Surf. Sci. (1973), https://doi.org/10.1016/0039-6028(73)90337-3.

[31] J. Krustok, T. Raadik, M. Grossberg, S. Giraldo, M. Neuschitzer, S. López-Marino, E. Saucedo, Temperature dependent electroreflectance study of Cu 2 ZnSnSe 4 solar cells, (2015). https://doi.org/10.1016/j.mssp.2015.04.055.

[32] M. Grossberg, J. Krustok, A. Jagomägi, M. Leon, E. Arushanov, A. Nateprov, I. Bodnar, Investigation of potential and compositional fluctuations in $CuGa_3Se_5$ crystals using photoluminescence spectroscopy, Thin Solid Films 515 (2007) 6204–6207, https://doi.org/10.1016/j.tsf.2006.12.068.

[33] D. Huang, C. Persson, Band gap change induced by defect complexes in Cu2ZnSnS 4, Thin Solid Films (2013), https://doi.org/10.1016/j.tsf.2012.10.030.

[34] T. Raadik, J. Krustok, M. Kauk-Kuusik, K. Timmo, M. Grossberg, K. Ernits, J. Bleuse, Low temperature time resolved photoluminescence in ordered and disordered Cu_2ZnSnS_4 single crystals, Phys. B Condens. Matter. 508 (2017) 47–50, https://doi.org/10.1016/j.physb.2016.12.011.

[35] M. Grossberg, J. Krustok, T. Raadik, M. Kauk-Kuusik, J. Raudoja, Photoluminescence study of disordering in the cation sublattice of Cu_2ZnSnS_4, Curr. Appl. Phys. 14 (2014) 1424–1427, https://doi.org/10.1016/j.cap.2014.08.013.

[36] M. Grossberg, T. Raadik, J. Raudoja, J. Krustok, Photoluminescence study of defect clusters in Cu2ZnSnS 4 polycrystals, Curr. Appl. Phys. (2014), https://doi.org/10.1016/j.cap.2013.12.029.

[37] Y. Kumagai, K. Harada, H. Akamatsu, K. Matsuzaki, F. Oba, Carrier-Induced Band-Gap Variation and Point Defects in Zn 3N 2 from First Principles, (n.d.). https://doi.org/10.1103/PhysRevApplied.8.014015.

[38] K.P. O'Donnell, X. Chen, Temperature dependence of semiconductor band gaps, Appl. Phys. Lett. 58 (1991) 2924–2926, https://doi.org/10.1063/1.104723.

[39] M. Parenteau, C. Carlone, Influence of temperature and pressure on the electronic transitions in SnS and SnSe semiconductors, Phys. Rev. B. (1990), https://doi.org/10.1103/PhysRevB.41.5227.